

This is the accepted manuscript version of the contribution published as:

Lihl, C., Douglas, L.M., **Franke, S.**, Pérez-de-Mora, A., Meyer, A.H., Daubmeier, M., Edwards, E.A., **Nijenhuis, I.**, Sherwood Lollar, B., Elsner, M. (2019):
Mechanistic dichotomy in bacterial trichloroethene dechlorination revealed by carbon and chlorine isotope effects
Environ. Sci. Technol. **53** (8), 4245 - 4254

The publisher's version is available at:

<http://dx.doi.org/10.1021/acs.est.8b06643>

1 **Mechanistic dichotomy in bacterial trichloroethene dechlorination revealed by**
2 **carbon and chlorine isotope effects**

3 Christina Lihl[†], Lisa M. Douglas[‡], Steffi Franke[§], Alfredo Pérez-de-Mora[†], Armin H. Meyer[†], Martina Daubmeier[†],
4 Elizabeth A. Edwards[¶], Ivonne Nijenhuis[§], Barbara Sherwood Lollar[‡] and Martin Elsner^{†,||,*}

5

6 [†] Institute of Groundwater Ecology, Helmholtz Zentrum München, Ingolstädter Landstrasse 1, 85764 Neuherberg,
7 Germany

8 [‡] Department of Earth Sciences, University of Toronto, Toronto, Ontario M5S 3B5, Canada

9 [§] Department for Isotope Biogeochemistry, Helmholtz-Centre for Environmental Research – UFZ,
10 Permoserstrasse 15, 04318 Leipzig, Germany

11 [¶] Department of Chemical Engineering and Applied Chemistry, University of Toronto, Toronto, Ontario, M5S 3E5,
12 Canada

13 ^{||} Chair of Analytical Chemistry and Water Chemistry, Technical University of Munich, Marchioninistrasse 17,
14 81377 Munich, Germany

15

16 *Corresponding author: E-mail: m.elsner@tum.de

17

18 **Keywords:**

19 isotope effects • reductive dehalogenases • *Dehalococcoides* • reaction mechanisms

20

21 Published as

22 Lihl, C., Douglas, L.M., Franke, S., Pérez-de-Mora, A., Meyer, A.H., Daubmeier, M., Edwards, E.A., Nijenhuis, I.,
23 Sherwood Lollar, B., Elsner, M.: Mechanistic dichotomy in bacterial trichloroethene dechlorination revealed by
24 carbon and chlorine isotope effects. Environ. Sci. Technol. 53, 4245-4254 (2019), DOI: 10.1021/acs.est.8b06643

25

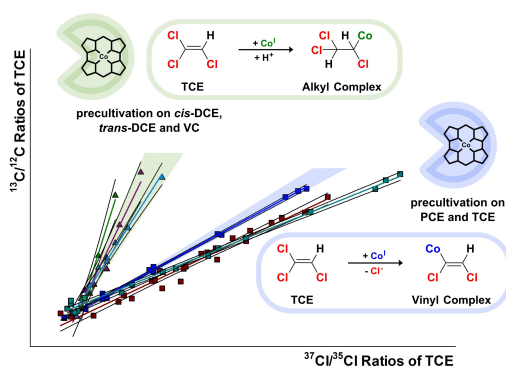
26 **Abstract:** Tetrachloroethene (PCE) and trichloroethene (TCE) are significant groundwater
 27 contaminants. Microbial reductive dehalogenation at contaminated sites can produce non-
 28 toxic ethene, but often stops at toxic *cis*-1,2-dichloroethene (*cis*-DCE) or vinyl chloride (VC).
 29 The magnitude of carbon relative to chlorine isotope effects – as expressed by $\Lambda_{C/Cl}$, the
 30 slope of $\delta^{13}C$ vs. $\delta^{37}Cl$ regressions – was recently recognized to reveal different reduction
 31 mechanisms with Vitamin B₁₂ as model reactant for reductive dehalogenase activity. Large
 32 $\Lambda_{C/Cl}$ values for *cis*-DCE reflected cob(I)alamin addition followed by protonation, whereas
 33 smaller $\Lambda_{C/Cl}$ values for PCE evidenced cob(I)alamin addition followed by Cl⁻ elimination. This
 34 study addressed dehalogenation in actual microorganisms and observed identical large $\Lambda_{C/Cl}$
 35 values for *cis*-DCE ($\Lambda_{C/Cl}$ = 10.0 to 17.8) that contrasted with identical smaller $\Lambda_{C/Cl}$ for TCE
 36 and PCE ($\Lambda_{C/Cl}$ = 2.3 to 3.8). For TCE, the trend of small $\Lambda_{C/Cl}$ could even be reversed when
 37 mixed cultures were precultivated on VC or DCEs and subsequently confronted with TCE
 38 ($\Lambda_{C/Cl}$ = 9.0 to 18.2). This observation provides explicit evidence that substrate adaptation
 39 must have selected for reductive dehalogenases with different mechanistic motifs. The
 40 patterns of $\Lambda_{C/Cl}$ are consistent with practically all studies published to date, while the
 41 difference in reaction mechanisms offers a potential explanation to the long-standing
 42 question of why bioremediation frequently stalls at *cis*-DCE.

43

44

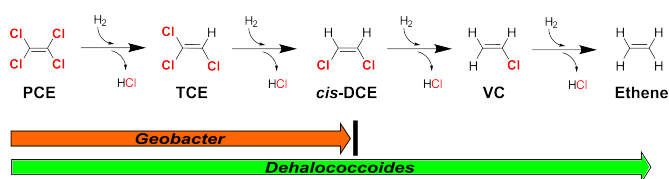
45 TOC Art:

46



47 **Introduction**

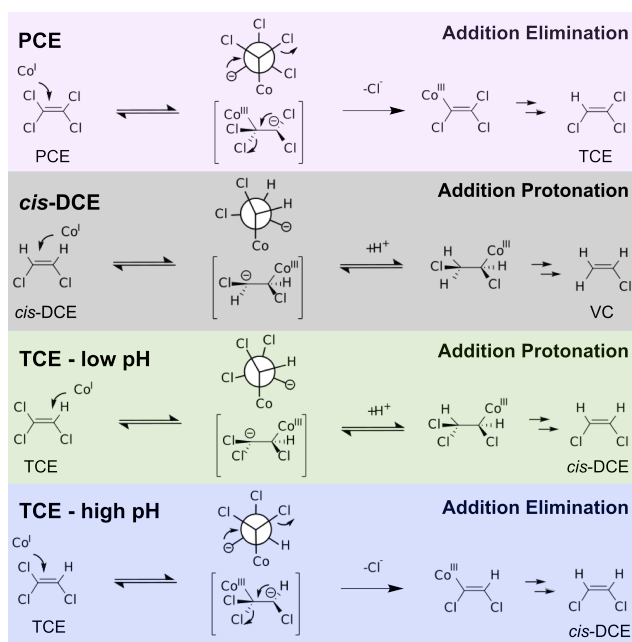
48 Chlorinated ethenes like tetrachloroethene (PCE) and trichloroethene (TCE), are among the
49 most frequent groundwater pollutants at contaminated sites worldwide¹. Under anoxic
50 conditions they may be reductively dechlorinated by microorganisms in a process known as
51 organohalide-respiration. Chloroethenes act as electron acceptors so that their C-Cl bonds
52 are reduced to C-H bonds (sequential hydrogenolysis) leading to non-toxic ethene as final
53 product (see Figure 1)². While this reaction stoichiometry is straightforward, the exact nature
54 of the underlying biochemical reaction mechanism has been elusive.



55 **Figure 1.** Reductive dechlorination of PCE to ethene with different end-points for two bacterial cultures.
56

57 Transformation frequently stalls at the stage of *cis*-1,2-dichloroethene (*cis*-DCE) or vinyl
58 chloride (VC) constituting one of the long-standing barriers to successful bioremediation of
59 these ubiquitous priority pollutants. Only specialized degrader strains – bacteria belonging to
60 the class *Dehalococcoidia* (e.g., certain *Dehalococcoides mccartyi* and *Dehalogenimonas*
61 strains) – were found to be capable of complete dechlorination to harmless ethene³⁻¹⁰. In
62 contrast, other microorganisms, such as *Geobacter lovleyi*, cannot dechlorinate beyond *cis*-
63 DCE⁴ (see Figure 1). Pinpointing the underlying mechanistic reasons, however, has
64 remained an elusive goal. Even though the catalytic site of all known reductive
65 dehalogenases (RDases) contains cobalamin as an essential Co(I)-containing corrinoid
66 cofactor, these enzymes occur in a great structural variety^{2, 4, 11-13}. Very few dehalogenase
67 protein structures have been solved yet^{11, 12}, and no reductive dehalogenase has been
68 uniquely characterized for its underlying biochemical transformation mechanism (i.e., bond
69 cleavage and formation). Consequently, critical research gaps in the chemistry of reductive
70 dechlorination exist: Is the mechanism the same for all substrates? Does the mechanism
71

72 correlate with a given substrate? Or do mechanisms vary with the observed variety of
 73 reductive dehalogenases and organisms?
 74 With reduced Vitamin B₁₂ as a chemical model system, we recently achieved a breakthrough
 75 in understanding reaction mechanisms *in vitro*¹⁴. Our evidence suggests that cob(I)alamin
 76 acts as a supernucleophile and adds to the double bond in chlorinated ethenes so that a
 77 carbanion complex is formed. If the free electron pair of this complex faces two vicinal Cl
 78 substituents (as in the reaction of PCE) one of them will be in *anti*-position, leading to fast
 79 elimination of Cl⁻ and producing a cobalamin chlorovinyl complex as short-lived intermediate
 80 (Scheme 1). In contrast, if there is only one vicinal Cl substituent (as in the reaction of *cis*-
 81 DCE) the molecular conformation is unfavorable for subsequent elimination so the carbanion
 82 is protonated instead. This results in a slower reaction pathway involving an intermediate
 83 chloroalkyl complex (Scheme 1). If there can be either one or two vicinal Cl substituents (as
 84 in the reaction of TCE) the addition-protonation pathway is favored at low pH, whereas the
 85 addition-elimination pathway is favored at high pH (Scheme 1). In contrast, the number and
 86 position of geminal Cl substituents does not seem to have an effect on the reaction
 87 mechanism.



88

89 **Scheme 1.** Reaction mechanisms for reductive dehalogenation of chlorinated ethenes via addition protonation or
 90 addition elimination (adapted from Heckel et al.¹⁴).

91

92 Both TCE dechlorination pathways eventually produce *cis*-DCE as the respective
93 hydrogenolysis product (Scheme 1) so that the different mechanisms are difficult to
94 distinguish from product analysis alone. Additional experimental evidence is, therefore,
95 warranted to determine whether the mechanistic dichotomy identified with Vitamin B₁₂ is also
96 at work in reductive dehalogenases or in dehalogenating organisms.

97 Compound-specific stable isotope effect measurements offer precisely such a
98 complementary line of evidence. Gas-chromatography (GC) coupled to isotope ratio mass
99 spectrometry (IRMS) measures carbon (¹³C/¹²C)^{15, 16} and chlorine (³⁷Cl/³⁵Cl) isotope ratios at
100 natural isotopic abundance¹⁷⁻¹⁹. Measured isotope ratios are expressed in the δ-notation, for
101 example for carbon:

$$102 \delta^{13}\text{C} = [({}^{13}\text{C}/{}^{12}\text{C})_{\text{Sample}} - ({}^{13}\text{C}/{}^{12}\text{C})_{\text{Reference}}] / ({}^{13}\text{C}/{}^{12}\text{C})_{\text{Reference}} \quad (1)$$

103 where (¹³C/¹²C)_{Reference} is the isotope ratio of an international reference material to ensure
104 comparability between laboratories^{20, 21}. An analogous equation applies to chlorine. When
105 correlating these isotope values of two elements relative to each other the regression slope

$$106 \Lambda_{\text{C/Cl}} = (\delta^{13}\text{C} - \delta^{13}\text{C}_0) / (\delta^{37}\text{Cl} - \delta^{37}\text{Cl}_0) \approx \epsilon_{\text{C}}/\epsilon_{\text{Cl}} \quad (2)$$

107 reflects the magnitude of the underlying compound-specific isotope effects during a
108 reaction²². Here δ^hE and δ^hE₀ are the isotope ratios of an element E (h = mass number of the
109 heavy isotope) at a given time and at the beginning of the reaction, respectively. Carbon and
110 chlorine enrichment factors (ε_C, ε_{Cl}) reflect compound-specific isotope effects²² that express
111 by how much molecules with heavy isotopes react slower than molecules with light
112 isotopes^{20, 23}. A value of ε = -10 ‰, for example, corresponds to a compound-specific
113 isotope effect of ¹²k/¹³k = 1.01 (for the experimental evaluation of ε see Eq. 3 below). Our
114 Vitamin B₁₂ study demonstrated that the slope Λ_{C/Cl} can provide a sensitive indicator of the
115 underlying reaction mechanisms in reductive chlorinated ethene dehalogenation with Vitamin
116 B₁₂¹⁴. Values of Λ_{C/Cl} were much larger in the addition-protonation mechanism, reflecting the
117 fact that no C-Cl bond was cleaved in the initial step so that chlorine isotope effects were
118 small. In contrast, values of Λ_{C/Cl} were smaller in the addition-elimination mechanism,

119 reflecting the larger chlorine isotope effect associated with C-Cl bond cleavage. When
120 compared to single element ϵ values, $\Lambda_{C/Cl}$ values have the additional advantage that the
121 slope $\Lambda_{C/Cl} = \epsilon_C/\epsilon_{Cl}$ remains remarkably constant even when intrinsic isotope effects show
122 variations.

123 The objective of this study was to analyze carbon and chlorine isotope effects during
124 reductive dehalogenation of chloroethenes with different bacterial cultures. The resulting
125 $\Lambda_{C/Cl}$ values were compared to the $\Lambda_{C/Cl}$ values of two mechanistic trends recently observed
126 in a Vitamin B₁₂ model system. To this end, we investigated in particular whether the isotope
127 fractionation trends in microbial dechlorination of *cis*-DCE and PCE correlate with trends of
128 the addition-protonation and the addition-elimination mechanism observed with Vitamin B₁₂,
129 respectively. For TCE dechlorination both mechanisms were observed in the Vitamin B₁₂
130 study depending on pH. To test whether evidence of both mechanisms may be observed for
131 TCE in living bacteria as well, microbial dechlorination of TCE was studied in seven different
132 experiments, either varying in precultivation substrate or in the type of predominant RDases
133 inside the bacteria. Finally, isotopic data of the dechlorination experiments of this study was
134 compared to literature data of available C/Cl isotope studies to test whether the picture of a
135 mechanistic dichotomy is consistent with published evidence to date.

136

137 **Material and Methods**

138 ***cis*-DCE and TCE dechlorinating cultures.** Dehalogenation experiments with *cis*-DCE
139 were carried out using *Dehalococcoides mccartyi* strain 195⁶ and the highly enriched
140 *Dehalococcoides mccartyi* strain BTF08 culture^{8, 24}. Dehalogenation experiments with TCE
141 were conducted with one pure culture (*Geobacter lovleyi* strain KB-1) and six mixed cultures
142 (KB-1/1,2-DCA, KB-1/VC, KB-1/cDCE, WBC-2/tDCE, KB-1 RF and Donna II) (see Table 1
143 for further details). *G. lovleyi* strain KB-1, KB-1/1,2-DCA, KB-1/VC and KB-1/cDCE and KB-1
144 RF were derived from KB-1, a commercially available enrichment culture, which is
145 specialized in the dehalogenation of chlorinated ethenes. It contains *G. lovleyi* strain KB-1
146 and a minimum of three strains of *Dehalococcoides*, as well as non-dechlorinating bacteria

147 like acetogens and methanogens²⁵⁻²⁹. Prior to the experiment the cultures were enriched on
148 different maintenance substrates for many years (see Table 1).

149 **Biotic dechlorination of *cis*-DCE under anoxic conditions with *D. mccartyi* strain 195**

150 **and strain BTF08.** *D. mccartyi* strain 195 was cultivated as described in Cichocka et al.³⁰

151 and Maymo-Gatell et al.⁶ with addition of butyrate pellets. *D. mccartyi* strain BTF08 was

152 cultivated following the protocol of Cichocka et al.⁸ and Schmidt et al.³¹. For each strain a set

153 of 23 serum bottles (50 ml) was filled with 25 ml anoxic medium and flushed with N₂ and CO₂

154 (70/30 %). After closing the bottles by crimping with Teflon[®] lined grey butyl rubber stoppers

155 they were sterilized for 40 min at 120 °C. Then they were spiked with *cis*-DCE (500 µM) as

156 electron acceptor and equilibrated overnight. On the next day the bottles were inoculated

157 with a culture grown on *cis*-DCE (2.5 % v/v for strain 195, 5 % v/v for strain BTF08). For

158 each set three non-inoculated bottles with substrate served as negative control. The bottles

159 were complemented with hydrogen as electron donor (0.5 bar overpressure). All cultures

160 were incubated in the dark without shaking at 20 °C (BTF08) or 30 °C (195). Progress of

161 substrate dehalogenation was monitored by concentration measurements with GC-FID. At

162 different levels of dechlorination bottles were sacrificed for analysis by stopping the

163 dechlorination reaction with 1 ml acidic sodium sulphate solution (280 g/l, pH ≈1) following

164 the protocol of Cichocka et al.³⁰. Samples were stored at 4 °C in the dark for later carbon

165 and chlorine isotope analysis via GC-IRMS.

166

167 **Table 1.** Summary of precultivation conditions, RDases and compound-specific isotope enrichment factors of carbon and chlorine.

Substrate for Dehalogenation and Isotope Analysis	Culture	Dechlorinators	Precultivation Substrate (electron donor)	Most abundant functional <i>rdhA</i> Genes*		Slope $\Lambda_{C/Cl}$ **	ϵ_{Cl} [‰]**	ϵ_C [‰]**	Duration
				before	after				
<i>cis</i> -DCE	<i>D. mccartyi</i> 195	<i>D. mccartyi</i> 195 (pure culture)	<i>cis</i> -DCE (hydrogen)	<i>tceA</i> ³²		10.0 ±0.4	-2.3 ±0.4	-23.2 ±4.1	no lag period, <i>cis</i> -DCE dehalogenation completed after one month
	<i>D. mccartyi</i> BTF08	<i>D. mccartyi</i> BTF08 (enrichment culture)	<i>cis</i> -DCE (hydrogen)	<i>tceA</i> ⁷		17.8 ±1.0	-1.7 ±0.4	-31.1 ±6.3	
TCE	<i>G. lovleyi</i> KB-1	<i>G. lovleyi</i> KB-1 (pure culture)	PCE (acetate)	<i>Geo-pceA</i> ³³		3.1 ±0.1	-3.3 ±0.3	-10.3 ±0.8	no lag period, TCE dehalogenation completed within one day
	KB-1 RF	multiple <i>D. mccartyi</i> strains (enrichment culture; no <i>Geobacter</i>)	TCE (methanol)	<i>vcrA</i> ³³		2.7 ±0.2	-3.3 ±0.3	-9.6 ±0.5	
	Donna II	<i>D. mccartyi</i> 195 (mixed culture; only one strain of <i>D. mccartyi</i>)	TCE (butyrate)	<i>tceA</i> ³⁴		2.3 ±0.1	-5.7 ±0.4	-13.5 ±0.6	
	KB-1/1,2-DCA	multiple <i>D. mccartyi</i> strains	1,2-DCA (methanol)	<i>tceA</i> ³⁵	<i>tceA</i> , <i>vcrA</i>	4.5 ±0.8	-1.2 ±0.3	-5.4 ±1.5	
	KB-1/VC	(enrichment cultures)	VC (methanol)	<i>vcrA</i> ³³	<i>vcrA</i>	18.2 ±4.3	-0.5 ±0.6	-10.6 ±9.3	
	KB-1/cDCE		<i>cis</i> -DCE (methanol)	<i>bvcrA</i> ³³ <i>vcrA</i>	<i>vcrA</i> (<i>tceA</i>)	11.8 ±2.4	-0.7 ±0.2	-8.3 ±3.4	
	WBC-2/tDCE	<i>Dehalogenimonas</i> sp., <i>D. mccartyi</i> (enrichment culture)	<i>trans</i> -DCE (lactate/ethanol)	<i>tdrA</i> (<i>Dhgm</i>), <i>vcrA</i> (<i>Dhc</i>) ₉	<i>vcrA</i> (<i>tceA</i> , <i>tdrA</i>)	9.0 ±1.1	-0.7 ±0.3	-7.0 ±1.9	

* the abundance of specific *rdhA* genes known to be present in the cultures was used as a way to track which of multiple strains grew in the mixed culture; *rdhA* genes in brackets were only detected in minor abundance; the KB-1 enrichments were selected because each harbored a different dominant expressed RDase initially

** ±95 % confidence intervals

168 **Biotic dehalogenation of TCE under anoxic conditions with *G. lovleyi* strain KB-1, KB-**
169 **1/1,2-DCA, KB-1/VC, KB-1/cDCE and WBC-2/tDCE.** Two hundred milliliters defined
170 mineral medium³⁶ and 55 μ l resazurin (0.4 %) were filled in glass bottles (250 ml).
171 Subsequently they were capped with Mininert™ valves (Supelco) and purged for 40 min with
172 a N₂/CO₂ gas mixture (80/20 %). Each bottle of *G. lovleyi* strain KB-1 was complemented
173 with 50 μ l acetate (1 M) and 9 μ l TCE, whereas each bottle of KB-1/VC, KB-1/cDCE, and
174 KB-1/1,2-DCA was complemented with 20 μ l methanol and 9 μ l TCE and each bottle of
175 WBC-2/tDCE was complemented with 22 μ l lactate solution (75 g/l), 44 μ l ethanol and 9 μ l
176 TCE. All substances and solutions for complementation were taken from anoxic stocks.
177 Afterwards all bottles were continuously agitated on an orbital shaker at 60 rpm at room
178 temperature for 24 hours for equilibration. Biotic dehalogenation started by inoculating each
179 bottle with 20 ml of active culture. In order to eliminate carryover of volatile organic
180 compounds the active cultures had been purged for one hour with a N₂/CO₂ gas mixture
181 (80/20 %). The bottles were prepared in triplicates for each culture. Furthermore, for each
182 culture non-inoculated bottles with substrate served as negative control and were monitored
183 alongside the experimental bottles. Five minutes after inoculation the first samples were
184 taken. The next samples were taken in intervals throughout the dehalogenation process. At
185 each sampling point 7 ml of liquid were removed from all the bottles. The sample of 7 ml was
186 then divided into 1 ml aliquots which were distributed into seven 1.5 ml glass vials and
187 closed with PTFE-lined screw-top caps. All samples were fixed with 50 μ l NaOH (1 M) to
188 stop biological activity. One of the seven vials was used for instant concentration analysis
189 which was performed on a GC-FID. The other six vials were frozen upside down for later
190 isotope analysis of carbon and chlorine performed via GC-IRMS^{37, 38}. Preparation of the
191 cultures (except the purging with N₂/CO₂) and taking samples was conducted in a glovebox
192 containing an anoxic atmosphere (80 % N₂, 20 % H₂).

193 **Biotic dehalogenation of TCE under anoxic conditions with KB-1 RF and Donna II.** The
194 whole experiment was conducted in a glovebox containing an anoxic atmosphere (80 % N₂,
195 10 % H₂, 10 % CO₂). Glass bottles (260 ml) were filled with 200 ml (KB-1 RF) or 210 ml

196 (Donna II) defined mineral medium³⁶ and inoculated with 20 ml (KB-1 RF) or 10 ml
197 (Donna II) active culture. Beforehand the cultures were purged with a N₂/CO₂ gas mixture for
198 30 min to eliminate carryover of volatile organic compounds. Triplicate experimental bottles
199 were capped with Mininert™ valves (Supelco) and complemented by adding 20 µl of
200 methanol (KB-1 RF), 8.75 µl butyrate (Donna II) and 9 µl of TCE. Furthermore, for each
201 culture non-inoculated bottles with substrate and killed control bottles (sterilized before TCE
202 addition) served as negative control and were monitored alongside the experimental bottles.
203 All replicates were continuously shaken at 350 rpm at room temperature (24 °C). At each
204 time point headspace samples were removed first for concentration measurements via GC-
205 FID and then for carbon isotope analysis via GC-IRMS. Subsequently 4 ml liquid samples
206 were removed and split into 1 ml aliquots. Liquid samples were acidified to a pH of < 2 with
207 50 µl of 1 M H₂SO₄ and closed with PTFE-lined screw-top caps and then frozen upside down
208 in 1.5 ml glass vials for later chlorine isotope measurements via GC-IRMS^{37, 38}. Sample
209 volumes removed were compensated with identical volumes of glovebox atmosphere to
210 maintain a constant pressure within the bottle. Septa inside the stopper of the Mininert™
211 vials were replaced after every second piercing to minimize leakage.

212 **Concentration measurements and carbon and chlorine isotope analysis.** Concentration
213 measurements via GC-FID and compound-specific isotope analysis of carbon and chlorine
214 via GC-IRMS were performed according to defined protocols (see SI).

215 **Evaluation of carbon and chlorine isotope fractionation.** Carbon and chlorine
216 enrichment factors (ϵ_C , ϵ_{Cl}) of *cis*-DCE and TCE dechlorination were calculated according to
217 the Rayleigh equation (Equation 3) using Sigma-Plot. The Rayleigh equation describes the
218 gradual enrichment of the residual substrate fraction f with molecules containing heavy
219 isotopes^{20, 22}, for example for carbon:

$$220 \ln [(\delta^{13}C+1) / (\delta^{13}C_0+1)] = \epsilon_C \cdot \ln f \quad (3)$$

221 The isotope ratios of carbon refer to certain time points, one of them at the beginning of an
222 experiment ($\delta^{13}C_0$). By plotting values of $\delta^{13}C$ vs. $\delta^{37}Cl$ (see Equation 2), dual element
223 isotope plots were obtained. These processes are also illustrated in Figure 2. 95 %

224 confidence intervals (CI) show the uncertainties of the calculated slopes $\Lambda_{C/Cl}$ ($\Delta\delta^{13}C/\Delta\delta^{37}Cl$).
225 In chemical reactions isotope effects occur predominantly at the reacting position. Therefore,
226 in many cases a position-specific apparent kinetic isotope effect (AKIE) may be estimated
227 under the assumption that there are no isotope effects at the other positions according to
228 $AKIE_{\text{position-specific}} = 1 / (n \cdot \epsilon_{\text{reacting position}} + 1)$ (4)
229 where n is the number of atoms in intramolecular competition²². However, for chlorinated
230 ethene reduction our mechanistic picture (Scheme 1) suggests that the situation is more
231 complex since isotope effects occur in different steps of the reaction sequence, and they
232 may occur at different positions of the molecule^{14, 39}. On the other hand, from IRMS
233 measurements alone intramolecular isotope effects are difficult to resolve. Thus, in this study
234 we decided not to estimate position-specific isotope effects but instead to report compound-
235 specific isotope effects in the form of ϵ values.

236 **qPCR (quantitative Polymerase Chain Reaction) analysis of KB-1/1,2-DCA, KB-1/VC,**
237 **KB-1/cDCE and WBC-2/tDCE.** qPCR analyses were conducted after the completion of the
238 TCE experiment. 8.5 ml sample of each culture were collected and subsequently 1.5 ml of
239 50 % glycerol were added. The samples were stored at -80 °C after freezing in liquid
240 nitrogen. For qPCR analysis 8 ml of each thawed sample were filtered through a sterile
241 0.22 μ M Sterivex filter (Millipore) using an Air Cadet Vacuum/Pressure Pump 400-1902
242 (Barnant Company). After filtration the Sterivex filters were immediately frozen at -80 °C. The
243 filters were removed from the filter casing, sliced into small pieces with a sterile surgical
244 blade and then transferred to a bead-beating tube. For DNA extraction the PowerSoil DNA
245 isolation kit (Mo Bio Laboratories Inc.) was used. The DNA was extracted by following the
246 manufacturer's protocol for maximum yields, except that DNA was eluted in 50 μ l sterile
247 UltraPure distilled water (Invitrogen) rather than in the eluent provided with the kit. By using
248 a spectrophotometer (NanoDrop ND-1000; NanoDrop Technologies) the DNA concentration
249 and quality were assessed. Afterwards the DNA samples were 10 times diluted with sterile
250 UltraPure distilled water. All subsequent steps were performed in a PCR cabinet (ESCO
251 Technologies). qPCR reactions were run in triplicates where each run was calibrated by

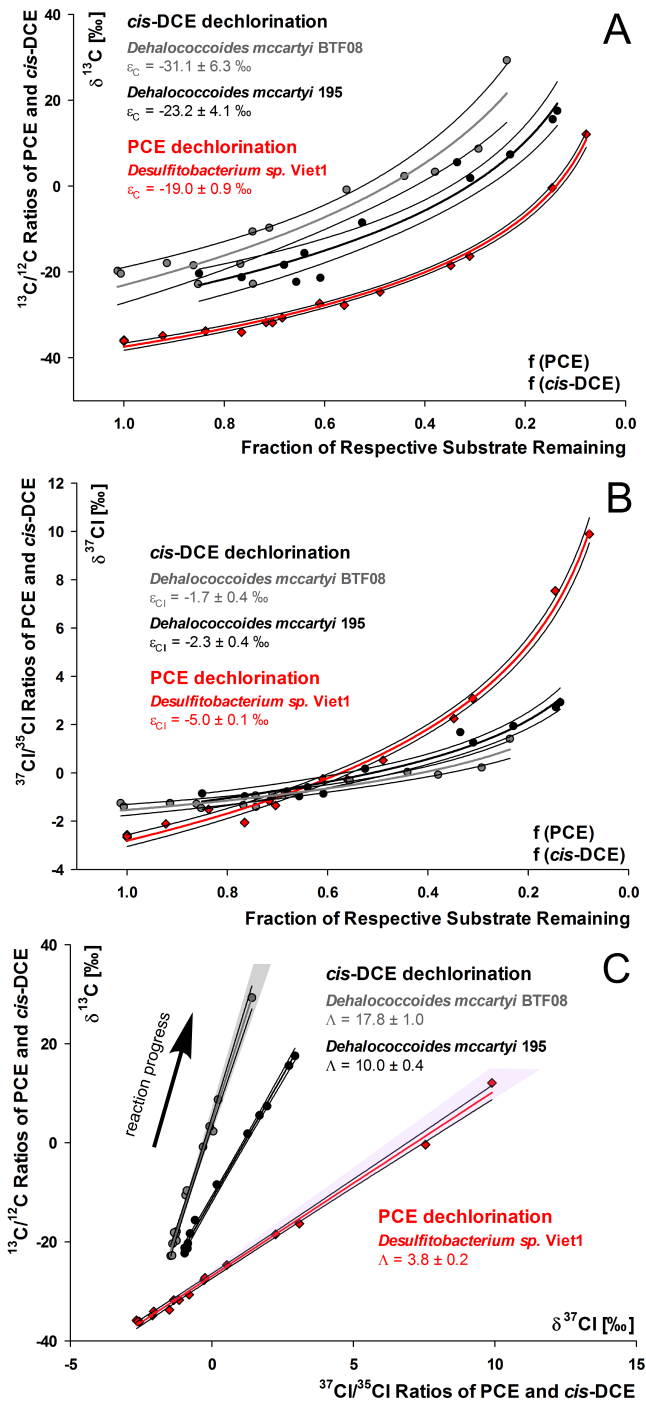
252 constructing a standard curve using known plasmid DNA concentrations containing the gene
253 insert of interest. The standard curve was run with eight concentrations ranging from 10 to
254 108 gene copies/ μ l. qPCR reaction solutions (20 μ l) were prepared in sterile UltraPure
255 distilled water containing 10 μ l of EvaGreen® Supermix, 0.5 μ l of each primer (forward and
256 reverse, each from 10 μ M stock solutions) and 2 μ l of diluted template (DNA extract or
257 standard plasmids). The qPCR reactions were conducted using a CFX96 real-time PCR
258 detection system with a C1000 Thermo Cycler using SsoFast™ EvaGreen® supermix (Bio-
259 Rad Laboratories). The thermocycling program started with the initial denaturation at 95 °C
260 for 2 min, followed by 40 cycles of denaturation at 98 °C for 5 s, annealing for 10 s (see
261 Table S1 in the SI for annealing temperatures), and a plate read. A final melting curve
262 analysis was conducted at the end of the program. The following genes were targeted by
263 qPCR using the defined primer sets (see Table S1 in the SI): the phylogenetic 16S rRNA
264 genes of *Dehalococcoides* and *Dehalogenimonas*, the functional genes *vcrA*, *tceA*, *bvcA*,
265 *tdrA*, as well as the 16S rRNA genes of total bacteria and total archaea.

266

267 **Results and Discussion**

268 **Starkly contrasting carbon and chlorine isotope fractionation suggests that microbial**
269 **dechlorination of *cis*-DCE and PCE follows different mechanisms.** To take advantage of
270 compound-specific isotope effects and evaluate whether the mechanistic dichotomy
271 observed *in vitro* can also be identified in pure strains of living organisms, we began with a
272 comparison between PCE and *cis*-DCE. Carbon and chlorine isotope values of *cis*-DCE
273 were measured in dehalogenation experiments with the strictly anaerobic organism
274 *Dehalococcoides mccartyi* strain 195⁶ and the highly enriched *Dehalococcoides mccartyi*
275 strain BTF08 culture^{8, 24}. Results were compared to our previous data on reductive
276 dechlorination of PCE by *Desulfitobacterium* sp. strain Viet1³⁹. Figure 2A and B show the
277 changes in carbon and chlorine isotope ratios with decreasing fraction of respective
278 substrate and the corresponding enrichment factors. Combining the isotope ratios of panel A

279 (carbon) and B (chlorine) leads to the formation of a dual element isotope plot as illustrated
 280 in panel C.
 281



282
 283 **Figure 2.** Carbon and chlorine isotope effects in reductive dehalogenation of *cis*-DCE by *D. mccartyi* BTF08
 284 (grey) and *D. mccartyi* 195 (black) and PCE by *Desulfitobacterium sp. Viet1* (red) (data from Cretnik et al.³⁹)
 285 resulting in a dual element isotope plot. (95 % confidence intervals are given as values and as black lines next to
 286 the regression slopes). (A) Carbon isotope fractionation and corresponding carbon enrichment factors ϵ_{C} . (B)

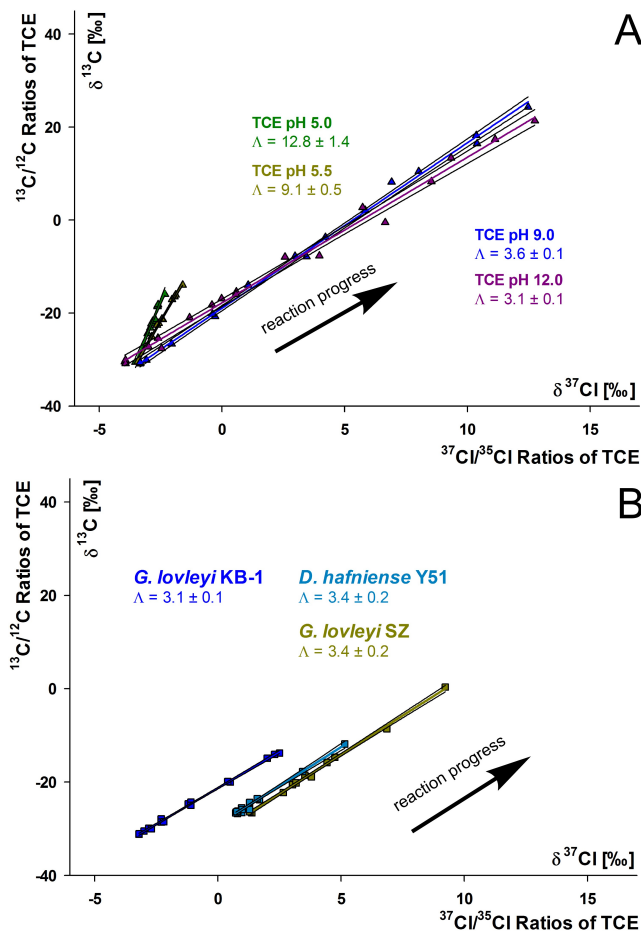
287 Chlorine isotope fractionation and corresponding chlorine enrichment factors ϵ_{Cl} . (Both ϵ evaluated according to
288 Eq. 3). (C) Resulting dual element isotope plots ($\delta^{13}\text{C}$ vs $\delta^{37}\text{Cl}$) indicate the occurrence of different underlying
289 transformation mechanisms corresponding to mechanisms observed with *cis*-DCE (shaded in grey) and PCE
290 (shaded in pink) by model reactions with Vitamin B₁₂¹⁴.

291

292 The dual element isotope trends with bacteria reproduced the trends obtained with Vitamin
293 B₁₂, and were reflected on the level of compound-specific carbon and chlorine isotope
294 effects, illustrated by ϵ_{C} and ϵ_{Cl} . Dechlorination of *cis*-DCE was associated with large carbon
295 and small chlorine isotope effects (*D. mccartyi* 195: $\epsilon_{\text{C}} = -23.2 \pm 4.1 \text{ ‰}$, $\epsilon_{\text{Cl}} = -2.3 \pm 0.4 \text{ ‰}$;
296 *D. mccartyi* BTF08: $\epsilon_{\text{C}} = -31.1 \pm 6.3 \text{ ‰}$, $\epsilon_{\text{Cl}} = -1.7 \pm 0.4 \text{ ‰}$) resulting in large dual element
297 isotope slopes $\Lambda_{195} = 10.0 \pm 0.4$ and $\Lambda_{\text{BTF08}} = 17.8 \pm 1.0$. In contrast, dechlorination of PCE
298 was associated with pronounced isotope effects in both elements ($\epsilon_{\text{C}} = -19.0 \pm 0.9 \text{ ‰}$,
299 $\epsilon_{\text{Cl}} = -5.0 \pm 0.1 \text{ ‰}$) giving rise to a smaller dual element isotope slope $\Lambda_{\text{Desulfitobacterium}} = 3.8$
300 ± 0.2 . This large chlorine isotope effect is even more striking when one considers that it is
301 averaged over four chlorine atoms in PCE (of which only one is cleaved off) while in *cis*-DCE
302 the average is taken over only two chlorine atoms. Hence, kinetic isotope effects of PCE and
303 *cis*-DCE at the reacting position (after correcting for the dilution by non-reacting chlorine
304 atoms) would show even greater differences⁴⁰. The same would be true for dual element
305 isotope slopes $\Lambda_{\text{C/Cl}}$. Our results therefore provide key lines of evidence suggesting that *cis*-
306 DCE and PCE must be dechlorinated via different mechanisms, and they exemplify the
307 pattern observed for addition-protonation vs. addition-elimination pathways (Scheme 1 and
308 Figure 2)¹⁴.

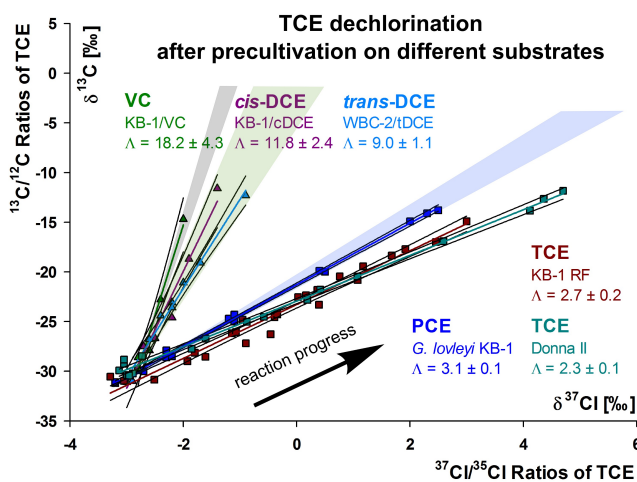
309 **Dual element isotope trends in TCE dechlorination by pure cultures are indicative of**
310 **an addition-elimination mechanism.** In an *in vitro* study using Vitamin B₁₂ as model
311 system TCE was recently observed to be dechlorinated via two different reaction
312 mechanisms depending on pH (see Figure 3A and Scheme 1). In order to probe which
313 mechanism would be observed for TCE *in vivo* with bacterial pure cultures, a *Geobacter*
314 subculture (*Geobacter lovleyi* KB-1) of the mixed consortium KB-1 that had been cultivated

315 to purity was investigated and compared to previously observed trends for *Geobacter lovleyi*
 316 SZ and *Desulfitobacterium hafniense* Y51³⁸ (Figure 3B). The dual element isotope slopes of
 317 the pure cultures correspond to the dual element isotope slopes of the Vitamin B₁₂ study at
 318 high pH values indicating that *in vivo* TCE is dechlorinated via the addition-elimination
 319 pathway.
 320



321
 322 **Figure 3.** Carbon and chlorine isotope effects in TCE reductive dehalogenation (A) by Vitamin B₁₂ at different pH
 323 values and (B) with pure cultures resulted in similar dual element isotope plots. (95 % confidence intervals are
 324 given as values and as black lines next to the regression slopes). (A) TCE reductive dehalogenation at high
 325 (green/yellow) and low (purple/blue) pH values (adapted from Heckel et al.¹⁴). (B) TCE reductive dechlorination
 326 with the pure culture *G. lovleyi* KB-1 (blue, this work) and the pure cultures *G. lovleyi* SZ (yellow) and
 327 *D. hafniense* Y51 (blue) (adapted from Cretnik et al.³⁸).
 328

329 **Precultivation of bacteria on less chlorinated ethenes leads to TCE dual element**
 330 **isotope trends indicative of an addition-protonation mechanism.** In order to investigate
 331 whether a different reaction mechanism can nonetheless be observed for TCE when using
 332 precultivation conditions to select for organisms with a different substrate preference, we
 333 conducted another set of experiments. Mixed cultures, Donna II and KB-1 RF, were
 334 precultivated on PCE or TCE for years (see Table 1), meaning that they were already
 335 adapted to TCE (substrate / daughter product of PCE dechlorination). On the other hand, we
 336 maintained another set of cultures on less chlorinated precultivation substrates: Three
 337 subcultures of the dechlorinating consortium KB-1 RF that were maintained on *cis*-DCE (KB-
 338 1/cDCE), VC (KB-1/VC) and 1,2-DCA (KB-1/1,2-DCA) for at least two years, and a fourth
 339 mixed culture that was enriched on *trans*-DCE (WBC-2/tDCE) for many years. As expected,
 340 cultures precultivated on TCE and PCE started to dechlorinate TCE immediately and the
 341 dechlorination was completed within one day (see Table 1). In contrast, the set of cultures
 342 enriched and precultivated on less chlorinated ethenes showed a lag period of 30-40 days
 343 before they started to dechlorinate TCE and dechlorination took 70-100 days for completion.
 344



345
 346 **Figure 4.** Dual element isotope trends indicate a mechanistic divide between TCE dechlorination by cultures
 347 precultivated on PCE (*G. lovleyi* KB-1, blue) and TCE (KB-1 RF, brown and Donna II, cyan) vs. cultures
 348 precultivated on VC (KB-1/VC, light green), *cis*-DCE (KB-1/cDCE, purple), and *trans*-DCE (WBC-2/tDCE, light
 349 blue). Shaded areas show the corresponding trends observed with *cis*-DCE (grey, pH 6.5) and TCE (green, low

350 pH/blue, high pH) in the Vitamin B₁₂ model¹⁴. (95 % confidence intervals are given as values and as black lines
351 next to the regression slopes).

352

353 Figure 4 shows that precultivation affected the carbon and chlorine isotope effects. A clear
354 divide appears between two dual element isotope trends depending on precultivation
355 conditions. Cultures precultivated on less chlorinated ethenes like VC (KB-1/VC), *cis*-DCE
356 (KB-1/cDCE) and *trans*-DCE (WBC-2/tDCE) showed large carbon isotope effects in
357 combination with small chlorine isotope effects corresponding to $\Lambda_{C/Cl}$ values between 9.0
358 and 18.2 ($\Lambda_{KB-1/VC} = 18.2 \pm 4.3$, $\Lambda_{KB-1/cDCE} = 11.8 \pm 2.4$, $\Lambda_{WBC-2/tDCE} = 9.0 \pm 1.1$). In contrast the
359 cultures *G. lovleyi* strain KB-1, KB-1 RF, and Donna II, precultivated on TCE or PCE,
360 showed significantly smaller $\Lambda_{C/Cl}$ values of 2.3 to 3.1 ($\Lambda_{Donna II} = 2.3 \pm 0.1$, $\Lambda_{KB-1 RF} = 2.7 \pm 0.2$,
361 $\Lambda_{G. lovleyi KB-1} = 3.1 \pm 0.1$) indicative of larger chlorine isotope effects. These results are similar
362 to the dual element isotope slopes $\Lambda_{C/Cl}$ observed for an addition-elimination mechanism with
363 Vitamin B₁₂. In contrast, cultures precultivated on less chlorinated substrates – *cis*-DCE (KB-
364 1/cDCE), VC (KB-1/VC), and *trans*-DCE (WBC-2/tDCE) – resulted in $\Lambda_{C/Cl}$ values of TCE
365 dechlorination that correspond to an addition-protonation pathway with Vitamin B₁₂.

366 Our observations suggest that in the bacterial cells a similar mechanistic dichotomy of
367 cob(I)alamin addition-elimination vs. cob(I)alamin addition-protonation took place as in the
368 model reaction with Vitamin B₁₂ at different pH (Scheme 1). In experiments with bacterial
369 cells, however, both the medium and the inside of the cells were buffered so that catalysis of
370 the different pathways must be effectuated by functional groups inside the enzymes' catalytic
371 sites. We therefore hypothesize that the enzyme architecture of RDases is tailored to
372 different specific reaction mechanisms, possibly due to the presence / absence of amino
373 acids with specific protonation functionalities.

374 **Mechanism-specific dual element isotope trends of TCE did not correlate with RDase**
375 **predominance.** Given that we observed evidence of different reaction mechanisms in
376 bacterial reductive dehalogenation of TCE, we further explored whether this mechanistic
377 dichotomy could be correlated with the predominance of specific reductive dehalogenases.

378 Therefore, three different bacterial cultures, that had been adapted to TCE and for which the
379 predominance of different RDases can be inferred (see Table 1), were compared. *G. lovleyi*
380 strain KB-1 has been shown to harbor only one RDase, *Geo-PceA*³³. For the mixed culture
381 KB-1 RF, the RDase *VcrA* is considered to be responsible for dechlorination³³. In the mixed
382 culture Donna II, *D. mccartyi* strain 195 is the organism responsible for dechlorination, and
383 the RDase *TceA* was identified as the most prominent dechlorinating enzyme³⁴.

384 The key outcome of this approach was that the dual element isotope plot of these three
385 cultures shows similar regression slopes ($\Lambda_{\text{Donna II}} = 2.3 \pm 0.1$, $\Lambda_{\text{KB-1 RF}} = 2.7 \pm 0.2$, $\Lambda_{\text{G. lovleyi KB-1}} = 3.1 \pm 0.1$, see Table 1 and Figure S2) for all three experiments, indicating that TCE was
387 dechlorinated via a similar chemical mechanism, irrespective of the type of RDase (*Geo-*
388 *PceA* vs. *VcrA* vs. *TceA*). The three slopes agree with those at high pH in the Vitamin B₁₂
389 study¹⁴, suggesting that in all three cases a sequence of addition-elimination was the
390 predominant reaction pathway.

391 Subsequently, quantitative polymerase chain reaction (qPCR) analysis was applied to detect
392 changes in the reductive dehalogenase gene (*rdhA*) composition when cultures that had
393 been precultivated on less chlorinated ethenes were adapting to TCE reductive
394 dechlorination (see Table 1). qPCR analysis indicated a significant shift in the culture KB-
395 1/cDCE after changing the electron acceptor from *cis*-DCE to TCE. Typically KB-1/cDCE is
396 dominated by the RDase *BvcA* when precultivated on *cis*-DCE³³. After the TCE
397 dechlorination experiment, however, the *rdhA* gene *bvcA* was no longer detected in the
398 qPCR analysis. Instead, the *rdhA* gene *vcrA* was most abundant, indicating that TCE
399 dechlorination was likely performed by a *vcrA*-containing strain of *Dehalococcoides*. For the
400 WBC-2/tDCE culture, only minor changes in the RDase composition were observed. Here
401 *vcrA* and *tdrA* genes were predominant before⁹ and after the experiment. WBC-2/tDCE
402 contains *Dehalogenimonas sp.*, which expresses *TdrA* for the dechlorination of *trans*-DCE to
403 VC⁹. Additionally, after the TCE dechlorination experiment a small number of *tceA* genes
404 were detected by qPCR. In case of KB-1/VC, no changes in the *rdhA* gene composition were
405 discernible. Before³³ and after the TCE dechlorination experiment with KB-1/VC, *vcrA* was

406 the most abundant RDase gene analyzed. The information obtained from the qPCR data
407 therefore suggests that the maintenance on one specific precultivation substrate has a
408 significant influence on the microbial community and the prevalence of RDase genes³⁵.
409 Nevertheless, isotope effects of all cultures still gave evidence of the same addition-
410 protonation mechanism (see Table 1 and Figure S2) suggesting that the reaction
411 mechanism was conserved in precultivated cultures even though shifts in the dominantly
412 expressed RDase were observed.

413 Finally, a comparison of Figure 4 and the qPCR data on predominant RDases (see Table 1
414 and Figure S2) suggests that there can be different mechanisms at work ($\Lambda_{\text{KB-1 RF}} = 2.7 \pm 0.2$
415 vs. $\Lambda_{\text{KB-1 VC}} = 18.2 \pm 4.3$) even though the same nominal RDase (VcrA) was predominant.
416 One possibility is that the VcrA dehalogenase complex in organisms adapted to less
417 chlorinated substrates is different from those enriched on TCE. Kublik et al.⁴¹ showed that in
418 *Dehalococcoides* the reductive dehalogenase is part of a complex containing a variety of
419 proteins. Potentially, these other electron transport proteins may affect the enzyme and its
420 isotope fractionation. Also the role of corrinoid prosthetic groups, which can affect
421 dechlorination^{13, 42}, has to be further investigated, since it was unclear what types of
422 corrinoids were produced in the mixed cultures. Another possibility is that the RDase
423 catalyzing the dechlorination in the non-TCE-adapted cultures is not VcrA, even though the
424 strains contained that gene. Quantitative polymerase chain reaction can only reveal that
425 genes containing *vcrA* became more abundant after switching the electron acceptor, but
426 qPCR cannot provide direct information about whether the RDase were actually expressed.
427 For example, Heavner et al.⁴³ pointed out that in all *Dehalococcoides*, and particularly in KB-
428 1, a specific RDase (DET 1545 homolog) shows elevated expression upon stress.

429 The observation that the predominance of nominal RDases did not correlate with isotope
430 effect trends therefore highlights the need for a complementary approach to classify
431 degradation in natural and engineered systems: not only based on the (meta)genomic
432 detection of RDase genes, but also based on dual element (C, Cl) isotope fractionation as
433 indicator of underlying (bio)chemical transformation mechanisms. For transformation of TCE

434 with different pure corrinoid cofactors, dual element isotope slopes between 3.7 and 4.5
435 were recently observed⁴⁴, which we may now interpret as indicative of an addition-
436 elimination mechanism.

437 **Previously observed stable isotope fractionation is consistent with the mechanistic**
438 **dichotomy observed in this study.**

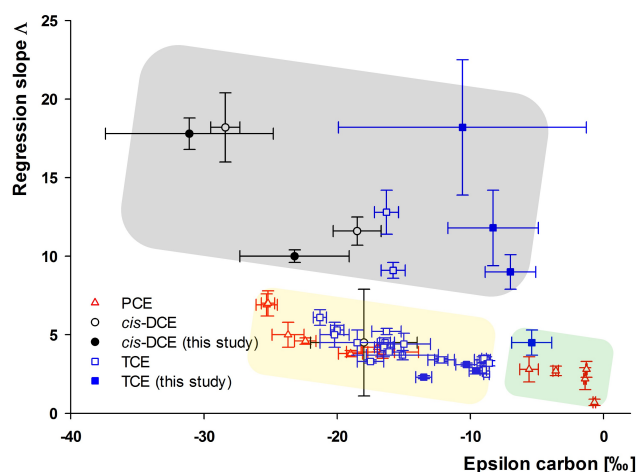
439 Figure 5 shows our data in the context of previously reported dual element isotope trends
440 $\Lambda_{C/Cl}$ in reductive dehalogenation by bacteria^{38, 39, 45-50}, in enzyme extracts⁴⁴, by pure
441 cofactors^{38, 44} or model systems^{14, 38}. To account for the potential effect of masking, these
442 values of $\Lambda_{C/Cl}$ are plotted against the corresponding carbon isotope enrichment factors ϵ_C ,
443 where pronounced negative ϵ_C indicate that intrinsic isotope effects are strongly expressed
444 meaning that the influence of masking is small. Vice versa, only slightly negative ϵ_C values
445 (corresponding to data points Figure 5, region shaded in green) indicate that intrinsic isotope
446 effects were strongly masked meaning that observable $\Lambda_{C/Cl}$ values did not necessarily
447 reflect the intrinsic biochemical reaction. Data points located in this putative masking-
448 dominated domain are derived from microbial degradation of PCE ($\Lambda_{C/Cl}$ values of 0.7 to 2.8
449 and slightly negative ϵ_C values of -0.7 ‰ to -5.6 ‰)^{44, 45, 50}, as well as from the TCE
450 dechlorinating culture KB-1/1,2-DCA ($\epsilon_C = -5.4 \pm 1.5$ ‰, $\Lambda_{KB-1/1,2-DCA} = 4.5 \pm 0.8$) of this study.
451 These smaller dual element isotope slopes potentially do not reflect the chemical bond
452 conversion but rather a preceding step (e.g., mass transfer into the cell, substrate-enzyme
453 binding, etc.)⁴⁴ and are, therefore, not discussed further here.

454 Pronounced negative ϵ_C , together with moderate $\Lambda_{C/Cl}$ values (Figure 5, region shaded in
455 yellow) are indicative of the addition-elimination mechanism¹⁴ brought forward in this study.
456 Indeed, microbial data in this domain^{38, 39, 45-48} originate almost exclusively from
457 dechlorination of PCE and TCE, including this study's data with cultures adapted to TCE
458 ($\Lambda_{Donna II} = 2.3 \pm 0.1$, $\Lambda_{KB-1 RF} = 2.7 \pm 0.2$, $\Lambda_{G. lovleyi KB-1} = 3.1 \pm 0.1$). Similar trends were observed
459 in transformation of TCE with enzymatic extracts⁴⁴ and purified cofactors^{38, 44} where all
460 values fell in a rather narrow experimental range ($\Lambda_{C/Cl} = 3.7 - 5.3$) indicating that the

461 predominance of an addition-elimination mechanism can be traced down to the enzyme
462 level¹⁴. An exception is a former *cis*-DCE degradation study ($\Lambda_{C/Cl} = 4.5$). The nature of this
463 degradation with field sediment rather than bacterial cultures was, however, little constrained
464 so that general conclusions are difficult⁴⁸.

465 In contrast, data points corresponding to pronounced negative ϵ_C , together with large $\Lambda_{C/Cl}$
466 values (Figure 5, region shaded in grey) are indicative of the addition-protonation
467 mechanism¹⁴. Indeed, all data are derived from either *cis*-DCE dechlorination (this and
468 previous^{48, 49} studies), or from TCE reductive dechlorination by cultures precultivated on less
469 chlorinated ethenes (this study). Taken together, the regions of Figure 5 confirm that also all
470 dual element isotope trends reported so far are consistent with the mechanistic dichotomy
471 observed in this study.

472



473

474 **Figure 5.** Carbon isotope fractionation factors ϵ_C and dual element isotope regression slopes $\Lambda_{C/Cl}$ in reductive
475 chlorinated ethene dehalogenation by bacteria^{38, 39, 45-50}, in enzyme extracts⁴⁴, by pure cofactors^{38, 44} or model
476 systems^{14, 38} observed in this study (filled symbols) and reported from previous studies (empty symbols).
477 Reductive dechlorination of PCE is depicted by red triangles, of TCE by blue squares and of *cis*-DCE by black
478 circles. (Error bars show 95 % confidence intervals of respective values). Shaded areas illustrate regions which
479 indicate that intrinsic isotope effects are masked (green), that they follow an addition-elimination mechanism
480 (yellow) or an addition-protonation mechanism (grey).

481

482 **Environmental Significance**

483 Available dual element isotope data reveal a surprising dichotomy in reductive dechlorination
484 chemistry of microbial communities. These results suggest that for dehalogenation of
485 chlorinated ethenes catalyzed by RDases two different reductive dechlorination mechanisms
486 exist, which are mimicked by the addition-elimination vs. addition-protonation pathways
487 identified in a recent Vitamin B₁₂ study¹⁴. The evidence that reductive dehalogenases may
488 be optimized to catalyze fundamentally different mechanisms, despite an identical net
489 reaction (hydrogenolysis), offer an explanation why some RDases can be specialized in the
490 dechlorination of PCE and TCE but cannot dechlorinate *cis*-DCE or VC. These results,
491 therefore, hold promise to potentially resolve a fundamental challenge to our understanding
492 of reductive dechlorination that has been a long-standing barrier to successful
493 bioremediation in the field – why dechlorination of chlorinated ethenes often stops at *cis*-
494 DCE or VC. A new RDase classification system based on catalyzed mechanisms may,
495 therefore, represent a transformative advance to the field in the future. Finally, this study
496 highlights the potential of dual element compound-specific stable isotope analysis as an
497 enabling technology to overcome a long-standing dilemma of organic (bio)chemistry: to
498 bridge the gap between *in vitro* and *in vivo*; to probe for reaction mechanisms in organisms;
499 and to directly observe a change of the involved RDases by detecting underlying
500 dechlorination mechanisms at contaminated sites.

501

502 **Associated Content**

503 Supporting Information

504 Concentration measurements via GC-FID, Figure depicting concentration vs. time for TCE
505 reductive dehalogenation, Figure depicting dual element isotope plots for TCE dechlorination
506 with regard to the predominant RDases, stable isotope analysis of carbon and chlorine via
507 GC-IRMS, Tables with detailed information regarding qPCR, Table with data of previous
508 studies used for Figure 5.

509 The Supporting Information is available free of charge.

510 **Acknowledgements**

511 This work was supported by the German National Science Foundation (DFG, Grants DFG
512 NI1323/2, EL 266/3-1 and EL 266/3-2) and the Natural Sciences and Research Council of
513 Canada. We thank Olivia Molenda and Katrina Chu who helped to run the experiments at
514 the University of Toronto.

515

516 **References**

517 (1) Bradley, P. M. Microbial degradation of chloroethenes in groundwater systems. *Hydrogeol. J.*
518 **2000**, *8*, (1), 104-111.

519 (2) Hug, L. A.; Maphosa, F.; Leys, D.; Löffler, F. E.; Smidt, H.; Edwards, E. A.; Adrian, L. Overview of
520 organohalide-respiring bacteria and a proposal for a classification system for reductive
521 dehalogenases. *Philos. Trans. R. Soc. London, Ser. B* **2013**, *368*, (1616), DOI: 10.1098/rstb.2012.0322.

522 (3) Taş, N.; Eekert, V.; Miriam, H.; De Vos, W. M.; Smidt, H. The little bacteria that can—diversity,
523 genomics and ecophysiology of ‘Dehalococcoides’ spp. in contaminated environments. *Microb.*
524 *Biotechnol.* **2010**, *3*, (4), 389-402.

525 (4) Smidt, H.; de Vos, W. M. Anaerobic microbial dehalogenation. *Annu. Rev. Microbiol.* **2004**, *58*,
526 43-73.

527 (5) Maymó-Gatell, X.; Anguish, T.; Zinder, S. H. Reductive dechlorination of chlorinated ethenes and
528 1, 2-dichloroethane by “Dehalococcoides ethenogenes” 195. *Appl. Environ. Microbiol.* **1999**, *65*, (7),
529 3108-3113.

530 (6) Maymo-Gatell, X.; Chien, Y.-T.; Gossett, J. M.; Zinder, S. H. Isolation of a Bacterium That
531 Reductively Dechlorinates Tetrachloroethene to Ethene. *Science* **1997**, *276*, (5318), 1568-1571.

532 (7) Pöritz, M.; Goris, T.; Wubet, T.; Tarkka, M. T.; Buscot, F.; Nijenhuis, I.; Lechner, U.; Adrian, L.
533 Genome sequences of two dehalogenation specialists—Dehalococcoides mccartyi strains BTF08 and
534 DCMB5 enriched from the highly polluted Bitterfeld region. In Blackwell Publishing Ltd Oxford, UK:
535 2013.

536 (8) Cichocka, D.; Nikolausz, M.; Haest, P. J.; Nijenhuis, I. Tetrachloroethene conversion to ethene by
537 a Dehalococcoides-containing enrichment culture from Bitterfeld. *FEMS Microbiol. Ecol.* **2010**, *72*,
538 (2), 297-310.

539 (9) Molenda, O.; Quail, A. T.; Edwards, E. A. Dehalogenimonas sp. strain WBC-2 genome and
540 identification of its trans-dichloroethene reductive dehalogenase, TdrA. *Appl. Environ. Microbiol.*
541 **2016**, *82*, (1), 40-50.

542 (10) Yang, Y.; Higgins, S. A.; Yan, J.; Şimşir, B.; Chourey, K.; Iyer, R.; Hettich, R. L.; Baldwin, B.; Ogles,
543 D. M.; Löffler, F. E. Grape pomace compost harbors organohalide-respiring Dehalogenimonas species
544 with novel reductive dehalogenase genes. *ISME J.* **2017**, *11*, (12), 2767-2780.

545 (11) Payne, K. A. P.; Quezada, C. P.; Fisher, K.; Dunstan, M. S.; Collins, F. A.; Sijts, H.; Levy, C.; Hay,
546 S.; Rigby, S. E. J.; Leys, D. Reductive dehalogenase structure suggests a mechanism for B12-
547 dependent dehalogenation. *Nature* **2015**, *517*, (7535), 513-516.

548 (12) Bommer, M.; Kunze, C.; Fessler, J.; Schubert, T.; Diekert, G.; Dobbek, H. Structural basis for
549 organohalide respiration. *Science* **2014**, *346*, (6208), 455-458.

550 (13) Yan, J.; Simsir, B.; Farmer, A. T.; Bi, M.; Yang, Y.; Campagna, S. R.; Löffler, F. E. The corrinoid
551 cofactor of reductive dehalogenases affects dechlorination rates and extents in organohalide-
552 respiring Dehalococcoides mccartyi. *ISME J.* **2016**, *10*, 1092-1101.

553 (14) Heckel, B.; McNeill, K.; Elsner, M. Chlorinated Ethene Reactivity with Vitamin B12 Is Governed
554 by Cobalamin Chloroethylcarbanions as Crossroads of Competing Pathways. *ACS Catal.* **2018**, *8*, (4),
555 3054-3066.

556 (15) Matthews, D. E.; Hayes, J. M. Isotope-Ratio-Monitoring Gas Chromatography-Mass
557 Spectrometry. *Anal. Chem.* **1978**, *50*, (11), 1465-1473.

558 (16) Sessions, A. L. Isotope-ratio detection for gas chromatography. *J. Sep. Sci.* **2006**, *29*, 1946-1961.

559 (17) Shouakar-Stash, O.; Drimmie, R. J.; Frape, S. K. Determination of inorganic chlorine stable
560 isotopes by continuous flow isotope ratio mass spectrometry. *Rapid Commun. Mass Spectrom.* **2005**,
561 *19*, (2), 121-127.

562 (18) Bernstein, A.; Shouakar-Stash, O.; Ebert, K.; Laskov, C.; Hunkeler, D.; Jeannotat, S.; Sakaguchi-
563 Soder, K.; Laaks, J.; Jochmann, M. A.; Cretnik, S.; Jager, J.; Haderlein, S. B.; Schmidt, T. C.; Aravena, R.;
564 Elsner, M. Compound-Specific Chlorine Isotope Analysis: A Comparison of Gas
565 Chromatography/Isotope Ratio Mass Spectrometry and Gas Chromatography/Quadrupole Mass
566 Spectrometry Methods in an Interlaboratory Study. *Anal. Chem.* **2011**, *83*, (20), 7624-7634.

567 (19) Shouakar-Stash, O.; Drimmie, R. J.; Zhang, M.; Frape, S. K. Compound-specific chlorine isotope
568 ratios of TCE, PCE and DCE isomers by direct injection using CF-IRMS. *Appl. Geochem.* **2006**, *21*, (5),
569 766-781.

570 (20) Hunkeler, D.; Meckenstock, R. U.; Sherwood Lollar, B.; Schmidt, T.; Wilson, J.; Schmidt, T.;
571 Wilson, J. *A Guide for Assessing Biodegradation and Source Identification of Organic Ground Water*
572 *Contaminants using Compound Specific Isotope Analysis (CSIA)*; PA 600/R-08/148 | December 2008 |
573 www.epa.gov/ada; US EPA: Oklahoma, USA, 2008.

574 (21) Coplen, T. B. Guidelines and recommended terms for expression of stable-isotope-ratio and
575 gas-ratio measurement results. *Rapid Commun. Mass Spectrom.* **2011**, *25*, (17), 2538-2560.

576 (22) Elsner, M. Stable isotope fractionation to investigate natural transformation mechanisms of
577 organic contaminants: principles, prospects and limitations. *J. Environ. Monit.* **2010**, *12*, (11), 2005-
578 2031.

579 (23) Bigeleisen, J. Chemistry of Isotopes: Isotope chemistry has opened new areas of chemical
580 physics, geochemistry, and molecular biology. *Science* **1965**, *29*, 463-471.

581 (24) Kaufhold, T.; Schmidt, M.; Cichocka, D.; Nikolausz, M.; Nijenhuis, I. Dehalogenation of diverse
582 halogenated substrates by a highly enriched Dehalococcoides-containing culture derived from the
583 contaminated mega-site in Bitterfeld. *FEMS Microbiol. Ecol.* **2012**, *83*, (1), 176-188.

584 (25) Duhamel, M.; Wehr, S. D.; Yu, L.; Rizvi, H.; Seepersad, D.; Dworatzek, S.; Cox, E. E.; Edwards, E.
585 A. Comparison of anaerobic dechlorinating enrichment cultures maintained on tetrachloroethene,
586 trichloroethene, cis-dichloroethene and vinyl chloride. *Water Res.* **2002**, *36*, (17), 4193-4202.

587 (26) Duhamel, M.; Mo, K.; Edwards, E. A. Characterization of a highly enriched Dehalococcoides-
588 containing culture that grows on vinyl chloride and trichloroethene. *Appl. Environ. Microbiol.* **2004**,
589 *70*, (9), 5538-5545.

590 (27) Duhamel, M.; Edwards, E. A. Microbial composition of chlorinated ethene-degrading cultures
591 dominated by Dehalococcoides. *FEMS Microbiol. Ecol.* **2006**, *58*, (3), 538-549.

592 (28) Duhamel, M.; Edwards, E. A. Growth and Yields of Dechlorinators, Acetogens, and
593 Methanogens during Reductive Dechlorination of Chlorinated Ethenes and Dihaloelimination of 1,2-
594 Dichloroethane. *Environ. Sci. Technol.* **2007**, *41*, (7), 2303-2310.

595 (29) Hug, L. A. A Metagenome-based Examination of Dechlorinating Enrichment Cultures:
596 Dehalococcoides and the Role of the Non-dechlorinating Microorganisms. Ph.D. Thesis, University of
597 Toronto, Toronto, Ontario, Canada, 2012.

598 (30) Cichocka, D.; Imfeld, G.; Richnow, H.-H.; Nijenhuis, I. Variability in microbial carbon isotope
599 fractionation of tetra- and trichloroethene upon reductive dechlorination. *Chemosphere* **2008**, *71*,
600 (4), 639-648.

601 (31) Schmidt, M.; Lege, S.; Nijenhuis, I. Comparison of 1,2-dichloroethane, dichloroethene and vinyl
602 chloride carbon stable isotope fractionation during dechlorination by two Dehalococcoides strains.
603 *Water Res.* **2014**, *52*, (0), 146-154.

604 (32) Magnuson, J. K.; Romine, M. F.; Burris, D. R.; Kingsley, M. T. Trichloroethene reductive
605 dehalogenase from Dehalococcoides ethenogenes: Sequence of tceA and substrate range
606 characterization. *Appl. Environ. Microbiol.* **2000**, *66*, (12), 5141-5147.

607 (33) Liang, X.; Molenda, O.; Tang, S.; Edwards, E. A. Identity and Substrate Specificity of Reductive
608 Dehalogenases Expressed in Dehalococcoides-Containing Enrichment Cultures Maintained on
609 Different Chlorinated Ethenes. *Appl. Environ. Microbiol.* **2015**, *81*, (14), 4626-4633.

610 (34) Fung, J. M.; Morris, R. M.; Adrian, L.; Zinder, S. H. Expression of reductive dehalogenase genes
611 in Dehalococcoides ethenogenes strain 195 growing on tetrachloroethene, trichloroethene, or 2, 3-
612 dichlorophenol. *Appl. Environ. Microbiol.* **2007**, *73*, (14), 4439-4445.

613 (35) Pérez-de-Mora, A.; Lacourt, A.; McMaster, M. L.; Liang, X.; Dworatzek, S. M.; Edwards, E. A.
614 Chlorinated Electron Acceptor Abundance Drives Selection of Dehalococcoides mccartyi (D.
615 mccartyi) Strains in Dechlorinating Enrichment Cultures and Groundwater Environments. *Front.*
616 *Microbiol.* **2018**, *9*, (812), DOI: 10.3389/fmicb.2018.00812.

617 (36) Edwards, E. A.; Grbić-Galić, D. Complete mineralization of benzene by aquifer microorganisms
618 under strictly anaerobic conditions. *Appl. Environ. Microbiol.* **1992**, *58*, (8), 2663-2666.

619 (37) Elsner, M.; Couloume, G. L.; SherwoodLollar, B. Freezing To Preserve Groundwater Samples
620 and Improve Headspace Quantification Limits of Water-Soluble Organic Contaminants for Carbon
621 Isotope Analysis. *Anal. Chem.* **2006**, *78*, (21), 7528-7534.

622 (38) Cretnik, S.; Thoreson, K. A.; Bernstein, A.; Ebert, K.; Buchner, D.; Laskov, C.; Haderlein, S.;
623 Shouakar-Stash, O.; Kliegman, S.; McNeill, K.; Elsner, M. Reductive Dechlorination of TCE by Chemical
624 Model Systems in Comparison to Dehalogenating Bacteria: Insights from Dual Element Isotope
625 Analysis ($^{13}\text{C}/^{12}\text{C}$, $^{37}\text{Cl}/^{35}\text{Cl}$). *Environ. Sci. Technol.* **2013**, *47*, (13), 6855-6863.

626 (39) Cretnik, S.; Bernstein, A.; Shouakar-Stash, O.; Löffler, F.; Elsner, M. Chlorine Isotope Effects
627 from Isotope Ratio Mass Spectrometry Suggest Intramolecular C-Cl Bond Competition in
628 Trichloroethene (TCE) Reductive Dehalogenation. *Molecules* **2014**, *19*, (5), 6450-6473.

629 (40) Elsner, M.; Zwank, L.; Hunkeler, D.; Schwarzenbach, R. P. A new concept linking observable
630 stable isotope fractionation to transformation pathways of organic pollutants. *Environ. Sci. Technol.*
631 **2005**, *39*, (18), 6896-6916.

632 (41) Kublik, A.; Deobald, D.; Hartwig, S.; Schiffmann, C. L.; Andrades, A.; von Bergen, M.; Sawers, R.
633 G.; Adrian, L. Identification of a multi-protein reductive dehalogenase complex in D ehalococcoides
634 mccartyi strain CBDB 1 suggests a protein-dependent respiratory electron transport chain obviating
635 quinone involvement. *Environ. Microbiol.* **2016**, *18*, (9), 3044-3056.

636 (42) Men, Y.; Seth, E. C.; Yi, S.; Crofts, T. S.; Allen, R. H.; Taga, M. E.; Alvarez-Cohen, L. Identification
637 of specific corrinoids reveals corrinoid modification in dechlorinating microbial communities.
638 *Environ. Microbiol.* **2015**, *17*, (12), 4873-4884.

639 (43) Heavner, G. L.; Mansfeldt, C. B.; Debs, G. E.; Hellerstedt, S. T.; Rowe, A. R.; Richardson, R. E.
640 Biomarkers' Responses to Reductive Dechlorination Rates and Oxygen Stress in Bioaugmentation
641 Culture KB-1TM. *Microorganisms* **2018**, *6*, (1), DOI: 10.3390/microorganisms6010013.

642 (44) Renpenning, J.; Keller, S.; Cretnik, S.; Shouakar-Stash, O.; Elsner, M.; Schubert, T.; Nijenhuis, I.
643 Combined C and Cl Isotope Effects Indicate Differences between Corrinoids and Enzyme
644 (Sulfurospirillum multivorans PceA) in Reductive Dehalogenation of Tetrachloroethene, But Not
645 Trichloroethene. *Environ. Sci. Technol.* **2014**, *48*, (20), 11837-11845.

646 (45) Wiegert, C.; Mandalakis, M.; Knowles, T.; Polymenakou, P. N.; Aeppli, C.; Macháčková, J.;
647 Holmstrand, H.; Evershed, R. P.; Pancost, R. D.; Gustafsson, Ö. Carbon and Chlorine Isotope
648 Fractionation During Microbial Degradation of Tetra- and Trichloroethene. *Environ. Sci. Technol.*
649 **2013**, *47*, (12), 6449-6456.

650 (46) Buchner, D.; Behrens, S.; Laskov, C.; Haderlein, S. B. Resiliency of Stable Isotope Fractionation
651 ($\delta^{13}\text{C}$ and $\delta^{37}\text{Cl}$) of Trichloroethene to Bacterial Growth Physiology and Expression of Key Enzymes.
652 *Environ. Sci. Technol.* **2015**, *49*, 13230-13237.

653 (47) Kuder, T.; van Breukelen, B. M.; Vanderford, M.; Philp, P. 3D-CSIA: Carbon, Chlorine, and
654 Hydrogen Isotope Fractionation in Transformation of TCE to Ethene by a Dehalococcoides Culture.
655 *Environ. Sci. Technol.* **2013**, *47*, (17), 9668-9677.

656 (48) Doğan-Subaşı, E.; Elsner, M.; Qiu, S.; Cretnik, S.; Atashgahi, S.; Shouakar-Stash, O.; Boon, N.;
657 Dejonghe, W.; Bastiaens, L. Contrasting dual (C, Cl) isotope fractionation offers potential to

658 distinguish reductive chloroethene transformation from breakdown by permanganate. *Science of*
659 *The Total Environment* **2017**, 596–597, 169-177.

660 (49) Abe, Y.; Aravena, R.; Zopfi, J.; Shouakar-Stash, O.; Cox, E.; Roberts, J. D.; Hunkeler, D. Carbon
661 and Chlorine Isotope Fractionation during Aerobic Oxidation and Reductive Dechlorination of Vinyl
662 Chloride and cis-1,2-Dichloroethene. *Environ. Sci. Technol.* **2009**, 43, (1), 101-107.

663 (50) Badin, A.; Buttet, G.; Maillard, J.; Holliger, C.; Hunkeler, D. Multiple Dual C–Cl Isotope Patterns
664 Associated with Reductive Dechlorination of Tetrachloroethene. *Environ. Sci. Technol.* **2014**, 48, (16),
665 9179-9186.

666